Final Report: Coulman High Seismic Experiment 2010-2011

Douglas S. Wilson
Bruce Luyendyk
Christopher Sorlien
UC Santa Barbara
April 2012

Preface

This report describes field activities for the 2010-11 seismic experiment to improve constraints on velocity as a function of depth at proposed ANDRILL Coulman High (CH) drill site CH-1, at shot point 2240 on marine seismic line NBP0301-1A0 (Fig. 1). The experiment consisted of an east-west line of surface shots and receivers centered on the drill site along line 1A0 and a hydrophone a few meters above the sea floor. Main goals were to determine depths to significant unconformities at CH-1 including early Miocene RSU5A [*Decesari*, 2006] and the Oligocene Coulman High Major Unconformity (CHMU).

Field Experiment design (Luyendyk, Wilson, C. Sorlien UCSB, Stuart Henrys GNS, Paul Passmore REF TEK, Tim Parker, Bob Greschke PASSCAL)

A few ice shelf seismic experiments have been made in the past [e.g., *Beaudoin et al.*, 1992; *Eisen et al.*, 2010; *Hansaraj et al.*, 2007] but the 2010-11 CH experiment was the first to combine a snow surface experiment with a hydrophone located beneath the ice shelf a few meters above the sea floor.

The intended wide-angle-hydrophone (WAH) experiment design was for 50 shots at 50 m spacing west of CH-1 and 100 receivers at 25 m east of CH-1 for a total offset of about 5 km; this geometry comprises an expanding spread profile. A hydrophone deployed near the sea floor would record all the shots in a walk-away geometry. Seismographs were REF TEK Texan 125A-01 battery powered miniature seismographs. Each unit needed to be powered by a 3.6V DD lithium thionyl battery to operate at cold temperatures for a day or more. Geophones were Sercel model L40A 40Hz . The hydrophone rig was a REFTEK model 17 sensor at the end of a 1000 m cable made by Cortland Cable Co. That cable was connected to a REF TEK RT130 digital acquisition system.

Shot and Receiver Surveying (F. Rack UNL SMO, R. Levy GNS, Chris Stubbs UCSB)

The experiment line was flagged 17 November 2010, at sites anticipated to drift north over multichannel seismic (MCS) line 1A0 in early January. Equipment included moderate-precision GPS and survey tape and rope. The cloth survey tape intended for spacing out sites performed poorly in the strong winds encountered, so a heavier rope was marked for an intended spacing of 50 meters between shots. Subsequent precise GPS surveys, however, indicate that the actual marking of the rope was much closer to 49.1 m than 50 m.

Shot Hole Melting and Loading (D. Blythe UNL, SMO, RPSC)

The ANDRILL Science Management Office (SMO) borrowed and refurbished a mobile hot water (melt) drill from Ice Coring and Drilling Services (ICDS) at the University of Wisconsin. The WAH required the melting of shot holes for placing the explosive charges used in the survey; the holes needed to be drilled to a depth slightly below the firn/ice transition (~40m below surface) to ensure that the charges would be coupled to the ice for optimal transmission of the blast waves into the seafloor. Shot holes were drilled 12-17 December, each to a depth of 35 m. Each hole was loaded with a string of 8 Pentex PowerPlus (TM) P boosters with a total mass of 3.2 kg. For the main survey line, 51 shots sites were surveyed but only 50 loaded (skipping the 49th from center). Additionally 3 test shots and 2 triangulation shots (to locate hydrophone) were deployed. Holes were loaded a few weeks prior to planned shooting to allow the charges to be well frozen into the ice for better energy coupling.

Hydrophone deployment (SMO staff, R. Greschke, C. Stubbs)

The hole for hydrophone deployment (Hole #4, Fig. 1; ice thickness 261 m, freeboard 44 m, water depth 812 m; Craig Stewart, pers. Comm. 2011) was melted 2 January near receiver sites 19 and 20 (~500 m east from center). It was located east of CH-1 in order to receive seismic ray paths bottoming–out beneath it. Initial hydrophone deployment was attempted on 3 January with an anchor of about 5 kg. There was no sign the anchor reached bottom after deploying more than 100 m more cable than depth to bottom. After checking on cable strength, the hydrophone was redeployed the morning of 4 January using the ~32-kg 'rabbit' weight (generally used for clearing holes) as an anchor. This greater weight reached bottom without incident. The hydrophone cable was configured with the outer Kevlar strength member separated from the conducting cable 1.5 m from the end, with the anchor connected to the strength member and syntactic foam floats (borrowed from the SCINI ROV) connected to the hydrophone to keep it from bouncing on the sea floor.

Test shots (Wilson, Greschke, Stubbs, Ethan Marcoux RPSC)

Twelve receivers were deployed at three sites for recording test shots on the afternoon of 4 January. At each of three receiver sites 20, 60 and 100 (ranges 500 m, 1500 m, and 2500 m from center), combinations of 4.5-Hz and 40-Hz geophones recording at 250 and 500 samples per second were deployed. (Geophone frequency refers to natural oscillation frequency of the sensor, below which ground motion is not well recorded.) Test shots were fired at ranges of 400 m, 1000 m, and 2000 m from center (Fig. 1). Differences in the test combinations were subtle, so 40-Hz geophones were chosen for their tolerance of being deployed away from vertically, and a sample rate of 500/s was chosen in anticipation of favorable weather not leading to long shooting time that might fill the memory capacity of the Texan recorders.

Geophone deployment (R. Greschke PASSCAL, D. Wilson, C. Stubbs, SMO)

Aluminum disks approx 10 cm in diameter were attached horizontally to 40-Hz Sercel geophones by threading them beneath the 9-cm spikes, with hopes of improving coupling in snow. A total of 100 geophones were deployed 5 January at 25-m spacing in shallow holes (depth 25-40 cm) about 1 m south of the flagged receiver site, with snow packed firmly over the geophones and lightly over the Texan recorders.

Shooting (Bob Greschke, Ethan Marcoux RPSC)

Shooting proceeded quickly and uneventfully on the morning and early afternoon of 6 January. Shot times were recorded using a surface geophone sampled at 1000/s and low gain. With many available hands, geophone recovery proceeded rapidly that afternoon.

GPS survey post shoot (Graham Roberts SMO, UNAVCO)

Differential GPS surveying of receiver and shot locations at 100-200 m intervals proceeded during windows of opportunity 5-7 January using equipment from UNAVCO. The general order was receiver locations, data shot locations, and triangulation shot locations.

Data Quality (R. Greschke, D. Wilson)

Initial inspection of data records indicated successful recording on all nearly all receivers (Figs. 2-5). There was a minor problem with several Texan recorders ceasing to record during the experiment; two stopped before the first shot and seven stopped before the last shot. Shot 26 may have been a partial misfire, with about 25% of the amplitude of adjacent shots. Hydrophone data show significant background noise at frequencies of 4-20 Hz, possibly from distant generators (not at the camp), but with most of the experiment energy at 100-200 Hz, this noise is easily removed by high-pass filtering. Data at relatively long ranges show apparent wide-angle reflections arriving 0.3-0.4 s after the water-bottom echo (Figs. 2-4) or direct arrival (Fig. 5) that we use to improve our knowledge of seismic velocity in the sediments. Presenting the data in a stacked, expanding-spread midpoint gather compared with an MCS midpoint gather (Fig. 6) shows that these arrivals are reflections from the CHMU horizon as identified in MCS.

Velocity-Depth Model

Velocity Analyses (VELANS) of MCS data (C. Sorlien)

Prior to the WAH experiment velocity control at the drill sites was solely from velocity analyses (VELANS) of the 22 fold MCS data. Decesari [2006] performed semblance analyses at 1 km spacing for the marine survey including line 1A0. The aim of new work was to refine prior VELANS and obtain depth estimates to drilling targets. C. Sorlien redid the VELANS at a spacing of 250 m on 1A0, yielding 195 new

analyses of stacking and interval velocities. New analyses (spaced at 250 m) also were done on N-S line NBP0301-11A1 and E-W line NBP0301-2B, located to the north (Fig. 1). These additional analyses were done to understand the extent and consistency of a low velocity layer found below CHMU and reflections and velocities at greater depth. Particular attention was required for reflections below the CHMU. Doug Wilson worked with Sorlien to combine the seismic results from the WAH with new VELANS to produce a joint velocity model at CH-1 (see Sediments section below).

Ray Tracing Technique (D. Wilson)

The main objective of the WAH experiment was to improve velocity constraints by recording seismic energy that traveled greater horizontal distance in sediment than in the case of the near vertical paths of energy in MCS data. With the complications introduced by the ice layer, the approximations used in routine MCS velocity analysis (i.e. Dix equation) become unreasonable. Therefore we use the ray tracing technique of *Zelt and Smith* [1992] to predict the arrival times of reflection from the CHMU, with emphasis on wide-angle reflections arriving after direct-ice arrivals and before ground-roll arrivals, especially at ranges of 2.5-4 km. Our strategy was to assess a 2-D model for sediment velocity by predicting both MCS arrivals (high-angle reflections for RSU5, CHMU, and a deeper CHS1 reflector) and over-ice arrivals for wide-angle CHMU reflections. Obviously, the velocities at the top of the model differ, with water velocities for MCS data and ice velocities for over-ice data.

Ice and Water

The velocity model for the ice starts with boundaries from GPS and radar surveys. The top of the ice was set at a uniform 41 m above sea level. The bottom of the ice was based on airborne radar (Fig. 7), 210 mbsl at -2 km range, 219 mbsl at the center, and 222 mbsl at +1.5-2.5 km range. Depth to seabed was simplified from NBP0301 multibeam sonar results, mostly 810-815 mbsl (corrected for local water sound velocity), with greater depths at negative ranges (west). Seismic velocity within ice closely follows previous work on the Ross Ice Shelf [*Beaudoin et al.*, 1992; *Robertson and Bentley*, 1990] with a linear gradient in a firn layer from 1 km/s at the surface to 3.81 km/s at 20 mbsl, then a slight velocity decrease to 3.75 km/s at the base of the ice, resulting from increasing temperature with depth. Velocity within water below the ice (1.443-1.452 km/s) is based on Coulman High Site Survey season CTD results (T ~ -1.8°C, salinity ~34.6) from M. Williams (email communication, 2011).

The model for ice and water was tested with a set of 44 water-bottom reflection times with the full range of offsets up to about 3.2 km (Fig. 8), for which water-bottom arrivals can be clearly distinguished from the within-ice phases. With minor adjustment of parameters such as velocity at base of ice, the mean residual between observation and ray-trace prediction was reduced to 0.07 ms, with a standard deviation of 5.3 ms. All further adjustments to fit sub-bottom reflections were applied only to sub-bottom velocities.

Sediments

Velocity models within sediments were first set to be consistent with MCS CDP gathers (NBP0301 line 1A0) using ray tracing through water and sediment, then each successful sediment model was checked against over-ice wide-angle data substituting ice for the top of the water in subsequent ray tracing. As a range of reasonable depths to the CHMU reflector is considered more useful than a best-fit depth, the goal was to develop a pair of models in addition to the best-fit model, one faster with a deeper reflector and one slower with a shallower reflector, both of which reasonably satisfied high-angle MCS travel time data and wide-angle over-ice data.

Our best-fit model (Fig. 9) has a linear velocity gradient from 2500 to 3200 m/s from 173 to 575 mbsf (RSU5A to CHMU). The mean travel-time residual for 35 MCS reflections is +0.4 ms, and for 32 mostly wide-angle over-ice reflections the mean residual is +0.2 ms. Our deep-fast model (Fig. 10) has a uniform velocity of 3050 m/s between 174 and 619 mbsf (RSU5A and CHMU). The mean travel-time residual for MCS data is –3.0 ms, and for over-ice reflection data the mean residual is +6.6 ms. The contrasting shallow-slow model (Fig. 11) has a linear velocity gradient from 2400 to 3000 m/s from 169 to 547 mbsf (again RSU5A to CHMU). The mean residuals are +3.5 ms for MCS and –6.7 ms for over-ice arrivals. There is good evidence from MCS moveout and reflection polarity that the velocity below CHMU is somewhat lower than the velocity above, about 2500-2800 m/s, suggesting that the interpreted marine section below CHMU is at least 250 meters thick.

Comparisons of velocity models

The suite of velocity–depth functions at drill site CH-1 are shown in Figure 12. Fig. 9 is the preferred solution (Best) in this report. The Best model predicts that the CHMU at CH-1 is at 575 m below the sea floor. Also shown are two interval velocity solutions from semblance analyses; a preliminary one done in 2004 by *Decesari* [2006] at shot point 2258 and a more refined one by C. Sorlien (2011; this report) at shot point 2238; CH-1 is at shot point 2240 (i.e., the 2011 semblance analysis is 50 m west of CH-1). Also shown is the regionally smoothed interval migration velocity function used by *Decesari* [2006] to process the entire NBP0301 survey over Coulman High.

Ray trace models include one for faster-deeper solutions “Fig. 10” and another slowest velocities and shallow depth, “Fig. 11”, consistent with joint data analyses; these bracket the possible ranges of solutions determined by trial-and-error. The “Best” velocity ray trace model Fig. 9 is the result of optimized r.m.s. errors on MCS data and good fit of the model to snow surface, over-ice data. This approach recognizes that near-vertical reflections can be modeled much more robustly than wide-angle reflections from a concave reflector. The Best and shallow-slow models ascribe a gradient in the velocity functions but a step-wise variation in velocity for the deep-fast analysis (Fig. 11) also satisfies the data.

All 2011 models predict a slow velocity layer beneath the CHMU. The Sorlien 2011 MCS VELANS indicates higher interval velocities below CHMU at the edges of the narrow graben where CH-1 is located. These are partly artifacts related to dip

and expected because of pinchout or truncation of the low velocity layer at the graben edges.

The Decesari 2004 analysis was done in advance of drill site selection, and the 1-km VELANS spacing was a large amount of analysis not focused on the needs of planning for drilling. Velocities picked were consistently higher than the 2011 re-analyses done at higher resolution. In addition, the interval velocities (derived from stacking velocities) were routinely smoothed by Decesari (or Sorlien) in 2003-2005, in order to minimize artifacts during depth migration. Thus, the migration velocity model could have averaged out single slow velocity analyses. The low velocity interval seems well resolved on multiple new analyses on three different MCS profiles including lines 1A0, 11 and 2 (Fig. 1).

The 2011 MCS model predicts a faster deep layer at ~ 900 m below sea floor (~1.77 sec; ~1700 mbsl); the 2004 MCS model predicts it deeper. We are more confident of the depth to the layer than its velocity. New VELANS around the drill site on lines 1A0 and 11A1 all show reflections at ~1.8 and ~2.0 seconds. Because of low moveout at these times, interval velocity solutions for the deep layer vary, with a range from 3.1 to 3.9 km/sec at different locations. Nevertheless, the 2011 analyses of the MCS data support an increase in velocity near 1700 mbsl depth at CH-1.

Best practices and developments needed

Experiment design: The experiment acquired good quality data at both the snow surface seismographs and the sea floor hydrophone. The hydrophone performed well and without incident once proper cable weighting was determined. Given that a single hydrophone was deployed the walk-away geometry produced only a receiver gather and it is fundamentally not possible to create a mid-point gather as with the expanding spread over-ice survey. Because there are some signal/noise advantages to having a receiver at the sea floor an improved approach would be to deploy an array of hydrophones along a sea floor cable. This could be accomplished with two melt holes and an ROV that could pull the array from one hole to the other along the sea floor.

Shot and receiver spacing: The basic frequency of energy was about 125 Hz. Horizontal energy wavelength is about 30 m, greater than the station spacing. For steeper arrival used in the analyses, apparent wavelengths would be larger, closer to 40 m. To avoid spatial aliasing the station spacing should be 20 m or less. The spacing we used, 25 m, is adequate for ray trace studies on first arrivals, but too large for processing steps such as F-k filtering. This should be kept in mind for future surveys.

Surveying of line: Windy conditions made it difficult to use surveying tape to lay out the shot and station locations to the desired accuracy. This was remedied post –experiment by the use of precision GPS to survey these locations. That should be the standard procedure for future surveys on the snow surface.

Shot hole depth: Radar studies indicated the firn depth was about 40 m and the shot holes were melted to 35 m. This seemed to work. In future surveys radar

needs to be used to estimate firn depth beforehand as melting the shot holes is time and labor intensive.

Explosives size: These were adequate for target design (3.2 kg) but could be easily increased with some likely benefit in penetration. Doubling of the size would make the charges about 2 m long, which can be accommodated in 35 m shot holes.

Batteries for Texans: Cold operating temperatures and recording time for a day or longer made using standard alkaline D cells impractical. Laboratory research by PASSCAL determined that Lithium compound D cells would hold up under the experiment conditions. In the experiment these performed well for the 36-hour duration of experiment and are recommended for future use.

Noise environment: The experiment encountered low frequency hum from unknown (distant?) source(s) that was easily removed by filtering. Local workers moving about during critical times created occasional noise in the data. Recommended that all personnel be listening on radios for shot alerts so they can be still during recording time.

Communications during experiment: Hand held radios lost contact over the full length of the line (5 km). Recommend that the shooting snowmobile be fitted with a longer-range whip antennae so it can broadcast voice alerts for shots to team members and the camp personnel.

Conclusions

- A joint analysis of 2003 MCS (2011 VELANS) and 2011 over-ice seismic data yields a best estimate depth to the CHMU of 575 mbsf. An acceptable velocity model using slower velocities yields a depth of 547 m while an acceptable faster velocity model yields a depth of 619 mbsf.
- The analyses cannot resolve whether the velocity-depth functions are best described as linear gradients or as step-wise changes in velocity with depth. Both are acceptable.
- Above the CHMU, new MCS 2011 VELANS agrees largely with 2010-11 over-ice experiments and ray trace modeling.
- A ~250 m thick low velocity layer below CHMU at CH-1 is incorporated in ray trace models; it is also detected in 2011 VELANS on north-south line 11A1 that intersects line 1A0 and parallel line 2B 4.2 kms to the north. The low velocity layer appears to be restricted to the local graben containing CH-1.
- MCS lines 11 and 12 near CH-1, and line 1A0 through the CH-1 site, image gently dipping reflections below the low velocity layer. Interval velocity from stacking velocity of 1A0 suggests higher velocities for this deeper section, although accuracy is limited because the depth to these deep horizons compared to the maximum offset for the relatively short multichannel streamer does not produce enough moveout for a confident velocity solution.
- This experiment showed the over-ice method is better than a single sea floor hydrophone. It was feared originally that the snow surface data would have low signal-to-noise and weak arrivals and that the

hydrophone would have higher signal-to-noise. In fact the snow surface data proved very acceptable; the higher redundancy of the surface data (yielding receiver gathers) was thus a considerable advantage in the analyses.

Acknowledgements

Stuart Henrys (GNS) helped us with the experimental design. We are grateful for the assistance of Tim Parker at the IRIS PASSCAL facility for help in setting up this experiment and to Bob Greschke for operating equipment in the field. Paul Passmore of REF TEK designed the hydrophone rig and Cortland Cable provided the cable. Daren Blythe and personnel at the ANDRILL Science Management Office (SMO) rebuilt the shot hole drill for use in this experiment. Frank Rack (SMO) and Richard Levy (GNS) did the survey of the line before the experiment. Christopher Stubbs (UCSB) assisted in the field program. UNAVCO provided a precision GPS so the line could be re-surveyed afterwards. Raytheon PSC provided explosives transport and shooting of the experiment. Funding provided by subaward 25-0550-0004-0030 from Univ. Nebraska under NSF grant OPP ANT-0839108.

References

Beaudoin, B. C., U. S. t. Brink, and T. A. Stern (1992), Characteristics and processing of seismic data collected on thick, floating ice: Results from the Ross Ice Shelf, Antarctica, Geophysics, 57(10), 1359-1372.

Decesari, R. C. (2006), The Mesozoic and Cenozoic Depositional, Structural, and Tectonic Evolution of the Ross Sea, Antarctica, Ph.D. thesis, 232 pp, University of California, Santa Barbara.

Eisen, O., C. Hofstede, H. Miller, Y. Kristoffersen, R. Blenkner, A. Lambrecht, and C. Mayer (2010), A New Approach for Exploring Ice Sheets and Sub-Ice Geology, Eos, 91(46), 429-440.

Hansaraj, D., S. A. Henrys, T. R. Naish, and ANDRILL_MIS-Science_Team (2007), McMurdo Ice Shelf Seismic Reflection Data and Correlation to the AND-1B drill hole, in Antarctica: A Keystone in a Changing World - Online Proceedings of the 10th ISAES X, edited by A. K. Cooper and C. R. Raymond, pp. Extended Abstract 101, 103 p.

Robertson, J. D., and C. R. Bentley (1990), Seismic studies on the grid western half of the Ross Ice Shelf: RIGGS I and RIGGS II, in The Ross Ice Shelf: Glaciology and Geophysics, edited by C. R. Bentley and D. E. Hayes, pp. 55-86, American Geophysical Union, Washington, DC.

Zelt, C., and R. Smith (1992), Seismic travel time inversion for 2-D crustal velocity structure, Geophysical Journal International, 108, 16-34.

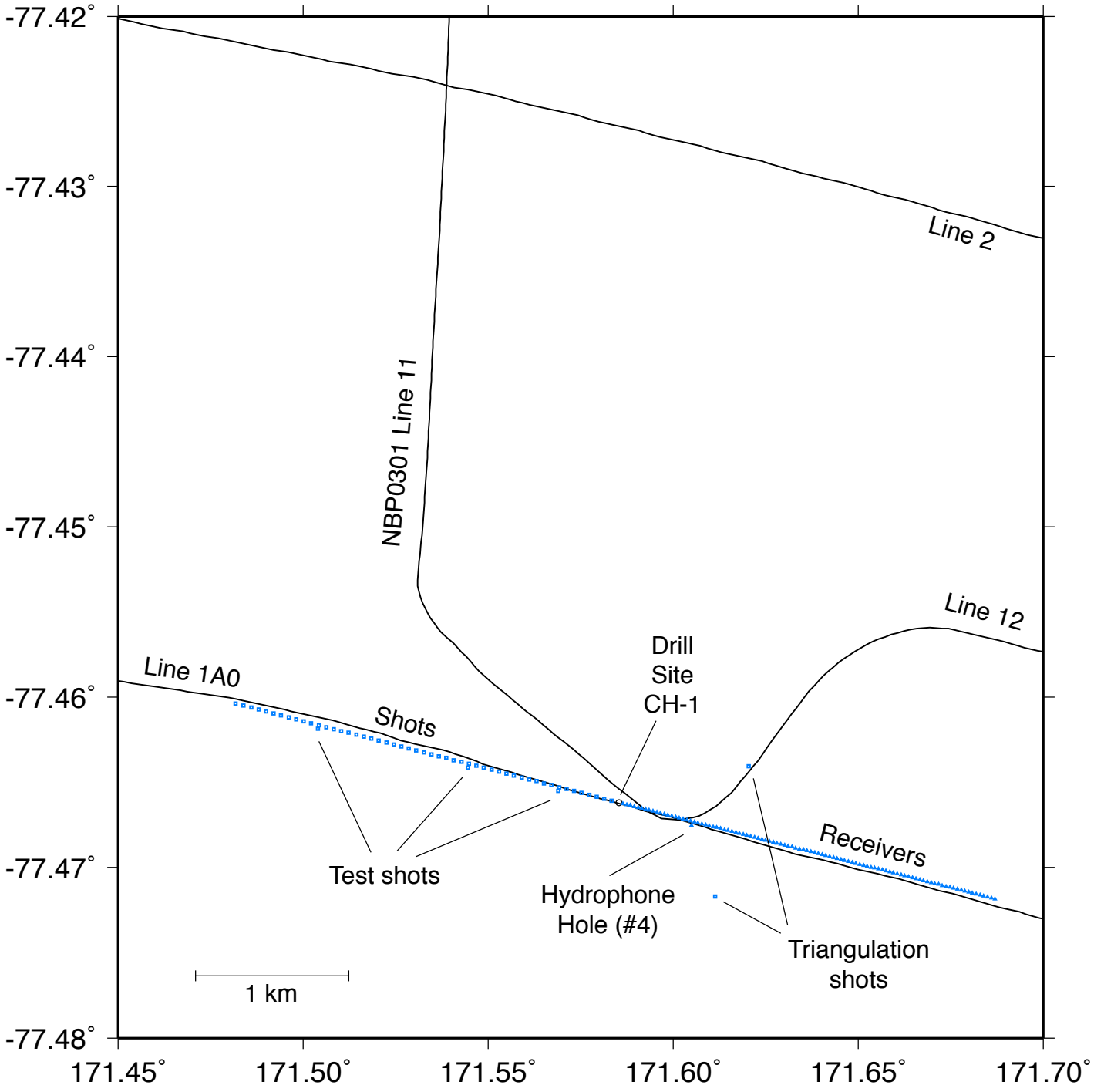

Figure 1. Location map for the Coulman High seismic experiment, showing NBP0301 seismic lines and early January positions of the elements of the experiment.

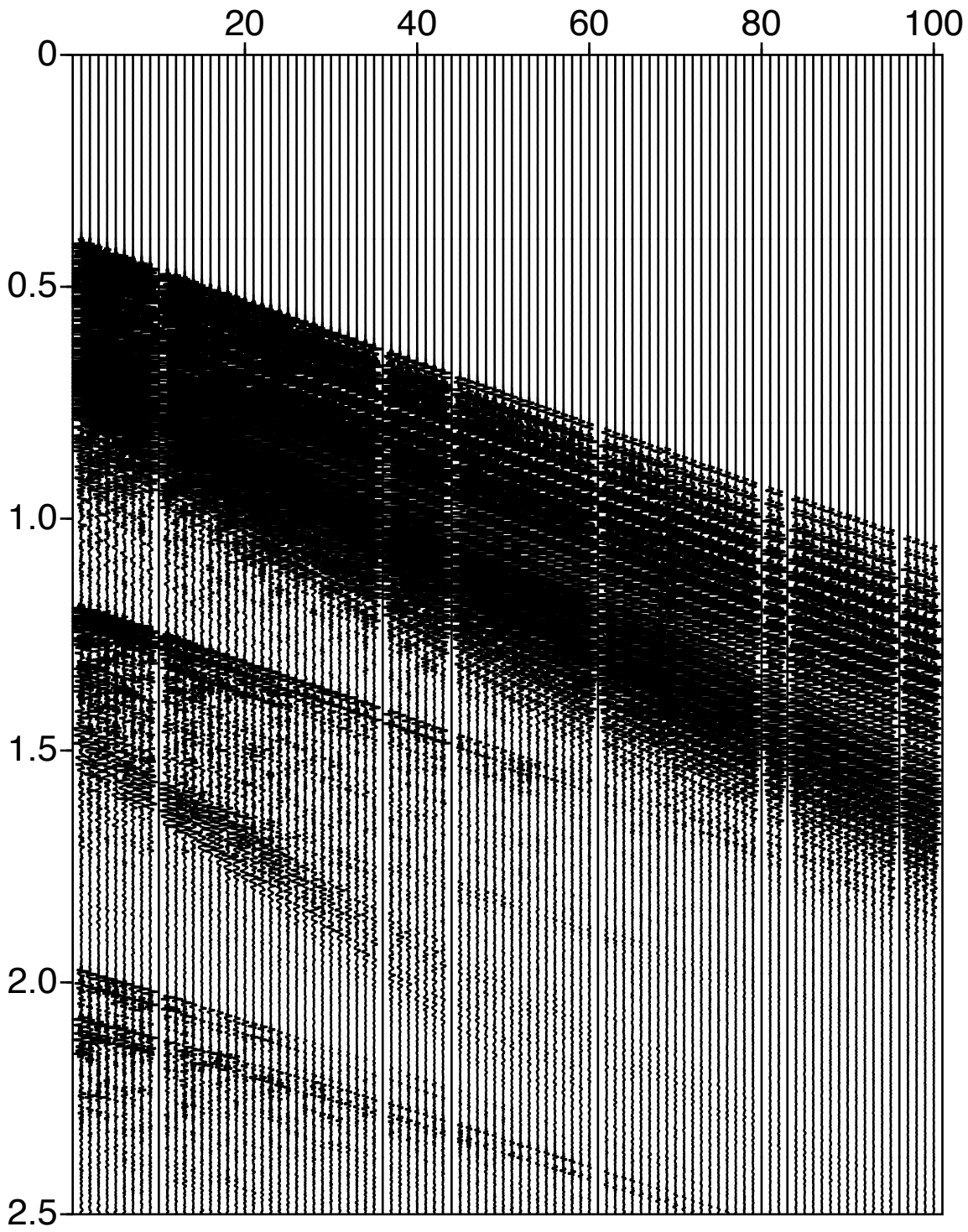

Figure 2. Shot gather for shot #30. The horizontal axis is labeled by receiver number, corresponding to ranges between 1525 and 4000 m. Vertical axis is travel time in seconds. No amplitude scaling

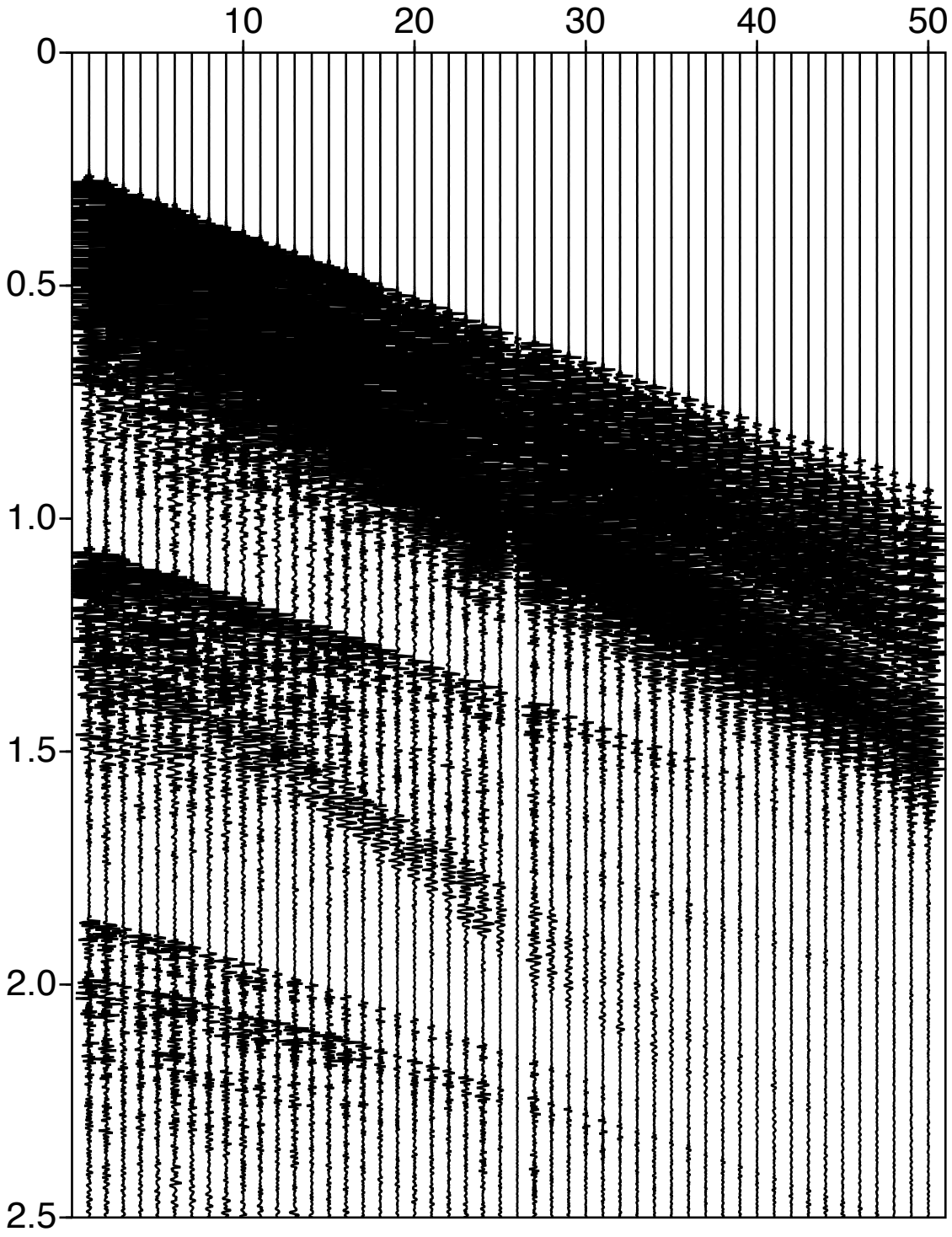

Figure 3. Receiver gather for geophone #40. The horizontal axis is labeled by shot number, corresponding to ranges between 1050 and 3500 m. Vertical axis is travel time in seconds. No amplitude scaling

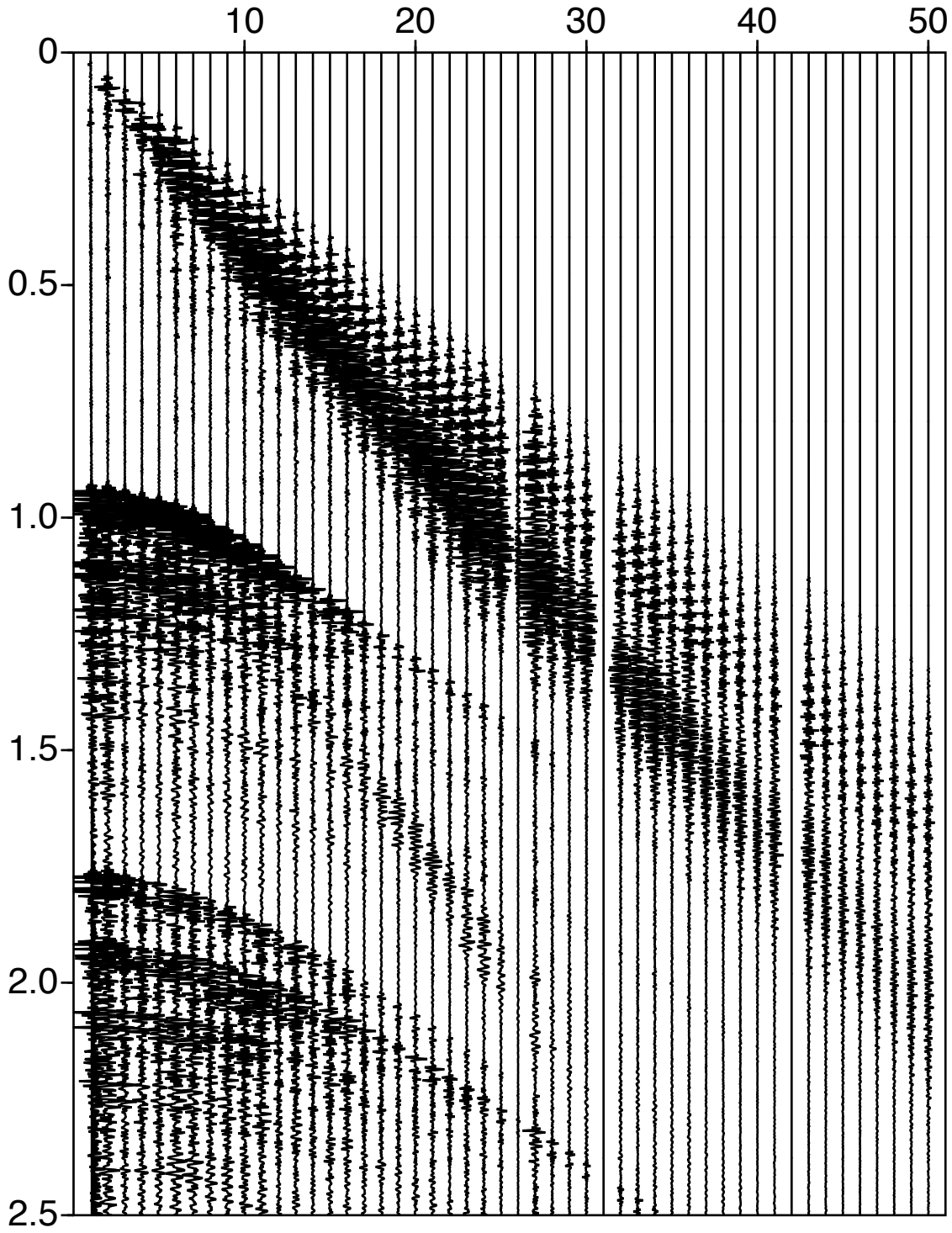

Figure 4. Expanding-spread (midpoint) gather for odd-numbered receivers. The horizontal axis is labeled by shot number, corresponding to ranges between 75 and 4975 m. Vertical axis is travel time in seconds. Amplitudes are scaled for spherical divergence.

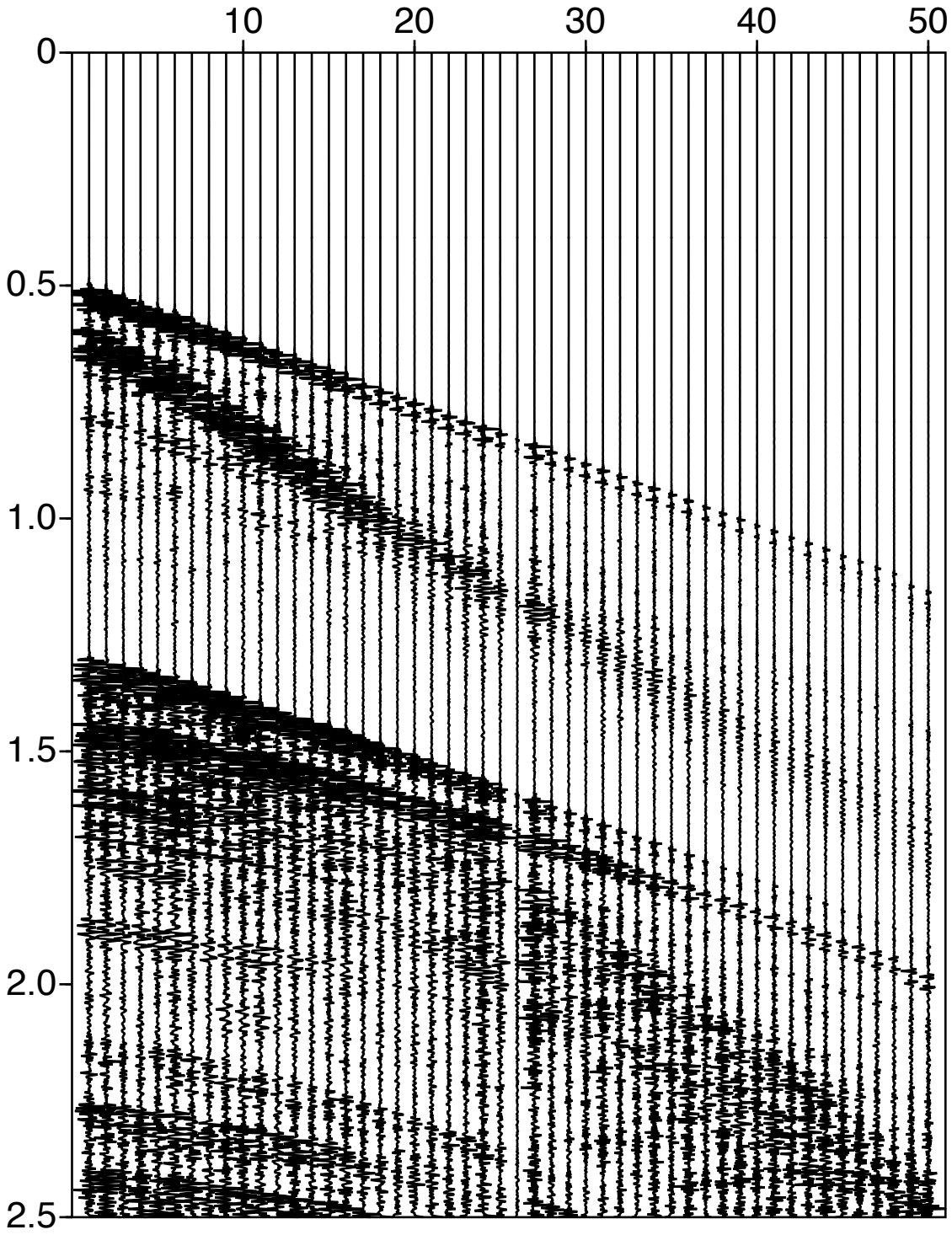

Figure 5. Hydrophone gather. The horizontal axis is labeled by shot number, corresponding to ranges between about 500 and 2950 m. Vertical axis is travel time in seconds. Data have been high-pass filtered to eliminate frequencies below 20 Hz and pass frequencies above 60 Hz. Amplitudes are scaled for spherical divergence.

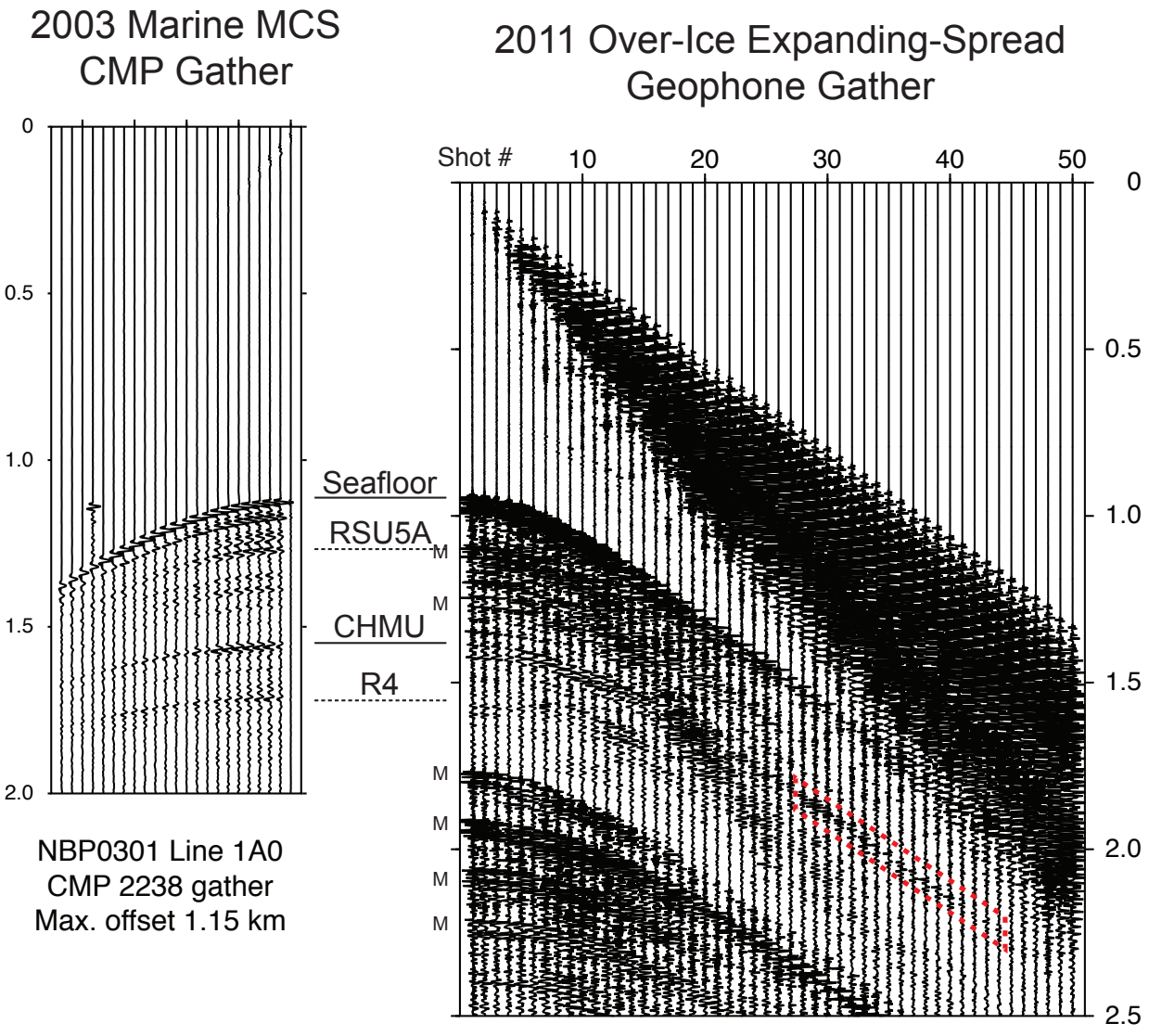

Figure 6. Midpoint gathers for MCS data (left) and over-ice data (right), centered near site CH-1. Each trace on the over-ice gather is a stack of up to 5 adjacent receivers, with a simple hyperbolic moveout to enhance reflected arrivals relative to direct-ice and ground-roll phases. The over-ice amplitudes are scaled for sperical divergence and trace balancing, with 'M's at near offset indicating multiple phases for within-ice and water-column reflections. The vertical shift between gathers aligns near-offset reflections accounting for high-velicty ice, and the MCS gather is mirrored relative to standard plotting conventions. The dashed red parallelogram highlights wide-angle CHMU reflections used for analyzing sediment velocities. RSU5A and R4 reflections are analyzed only in MCS data.

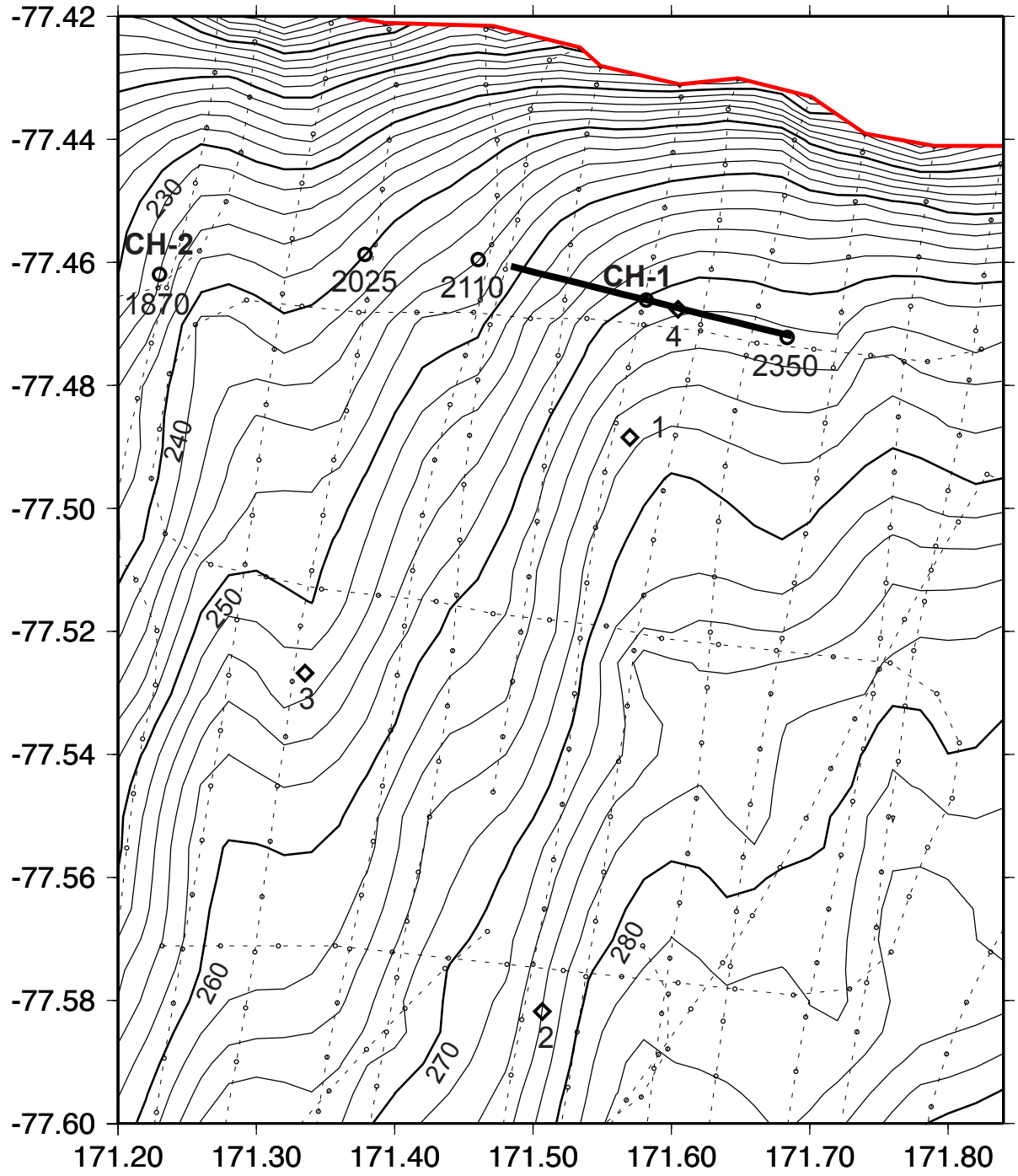

Figure 7. Contour map of ice thickness near the proposed CH drill sites, 2-m contour interval, constructed using airborne radar acquired December 2009 by CReSIS (Center for Remote Sensing of Ice Sheets; Claude Laird pers. comm. 2010). Flight lines are dashed, sampled generally at 1-km spacing (dots), then computer contoured. Bold straight line is location of CH WAH seismic experiment. Open circles are potential drill sites along marine MCS line 1A0; CH-1 and CH-2 are the preferred sites; other sites are labeled with their MCS shot point number. Diamonds mark locations of four melt holes made in the 2010-11 site survey season; hole 4 is where the hydrophone was lowered for this experiment.

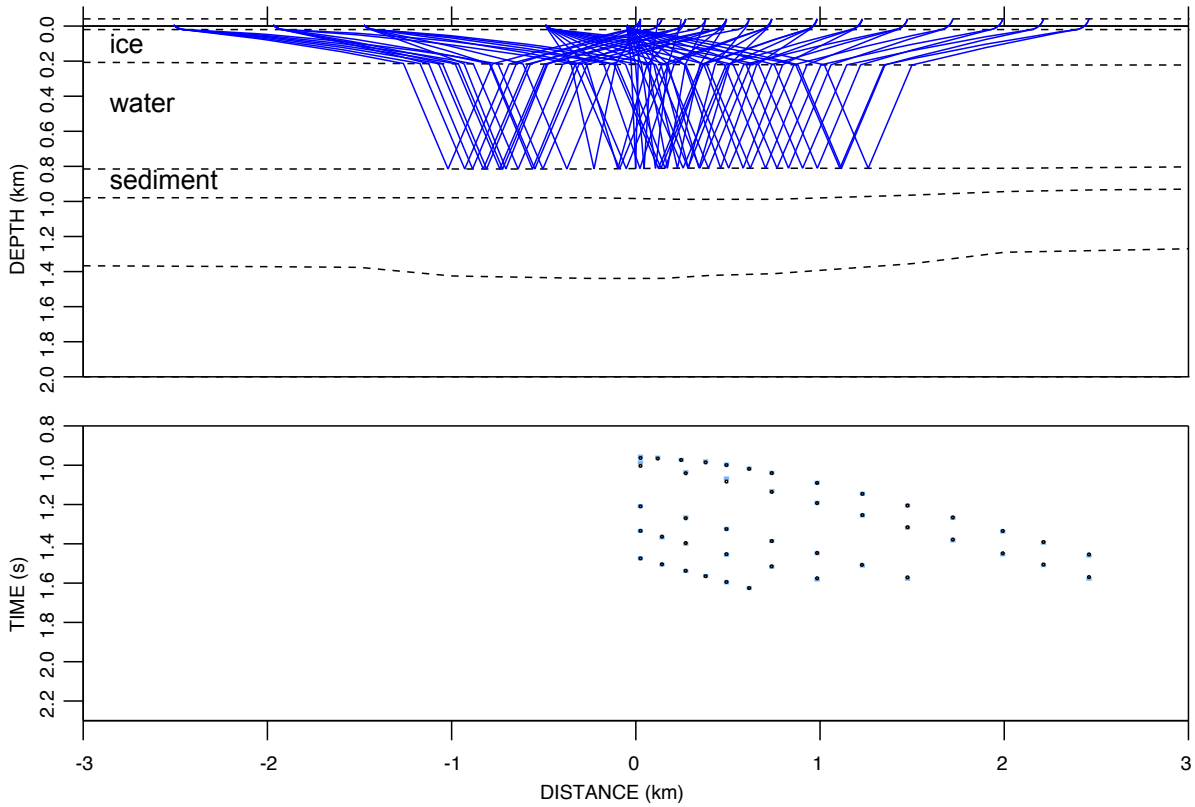

Figure 8. Ray-trace model for water-bottom reflections through ice. Upper panel shows ray paths; lower panels shows comparison of observed travel times (colored bars, ± 10 ms) and predicted times (black dots), plotted at the range of the receiver.

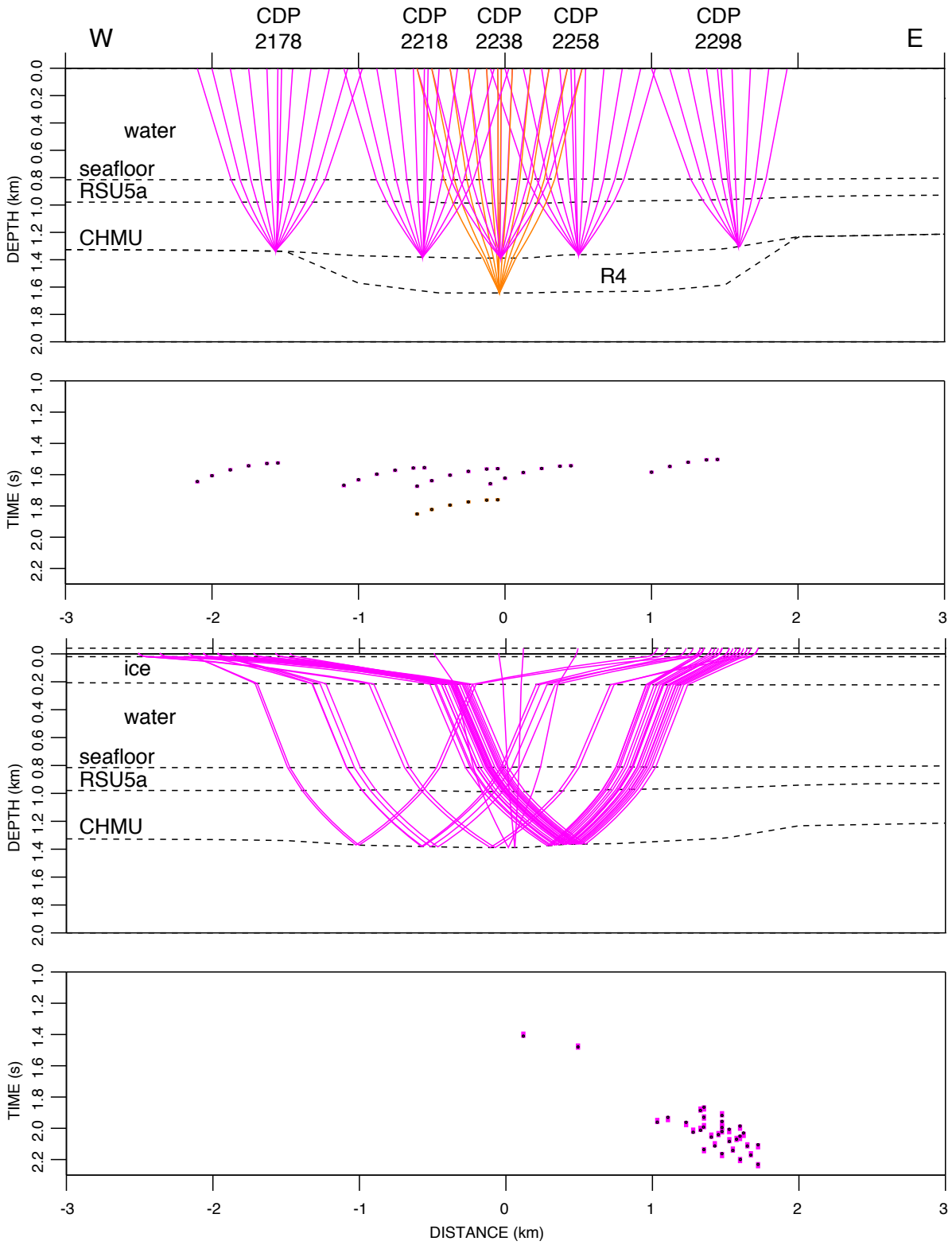

Figure 9. Ray-trace model for CHMU reflections near proposed drill site CH-1 for 2003 NBP0301 MCS data (top) and 2010 over-ice data (bottom). Colored bars for observed travel time are ± 10 ms for MCS and ± 20 ms for over-ice data. This model shows the best fit with CHMU at 575 mbsf. The MCS model also includes a deep reflector (R4) at 830 mbsf.

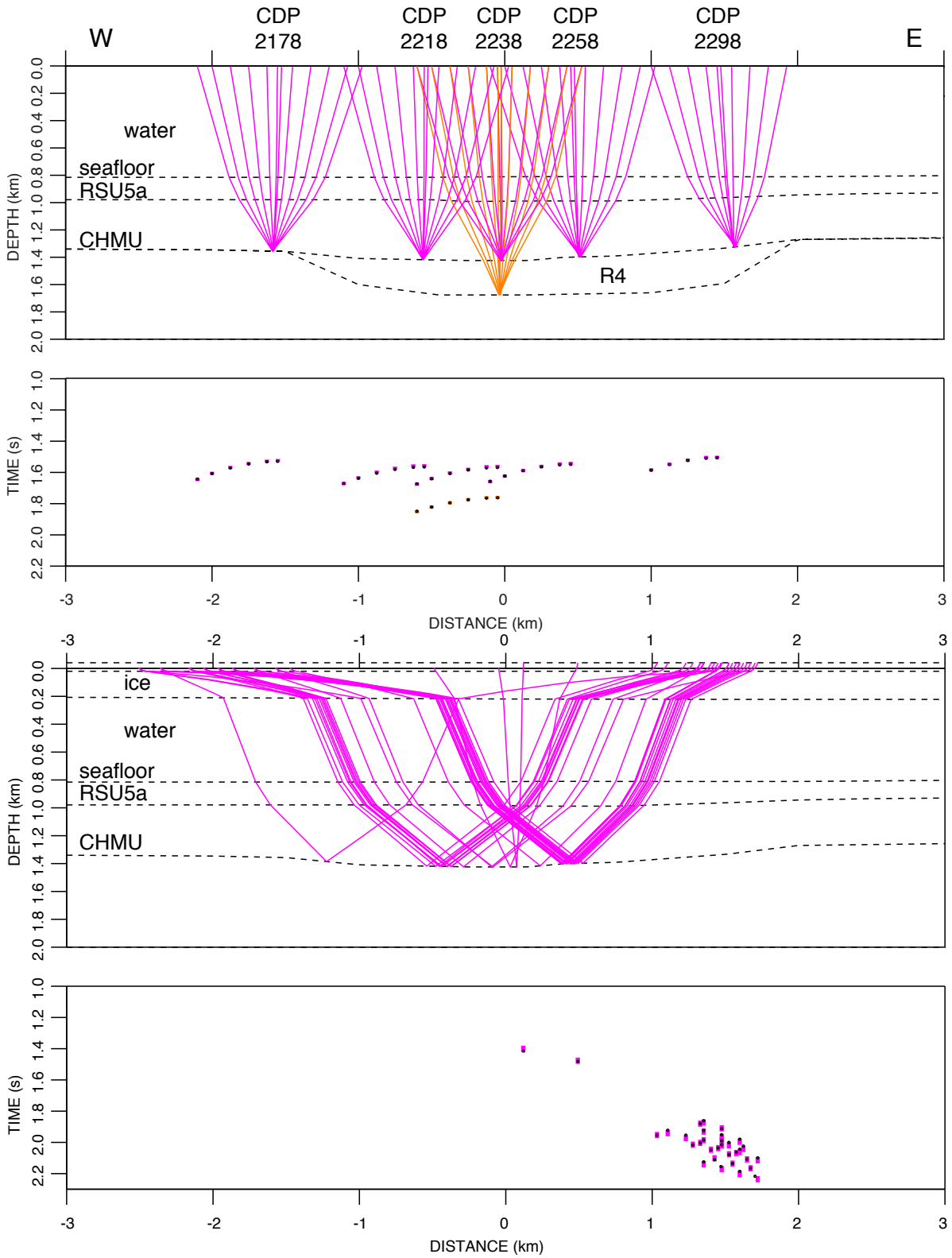

Figure 10. Ray-trace model for CHMU reflections near proposed drill site CH-1 for 2003 NBP0301 MCS data (top) and 2010 over-ice data (bottom). Colored bars for observed travel time are ± 10 ms for MCS and ± 20 ms for over-ice data. This model tests the fast and deep limit with CHMU at 619 mbsf. The MCS model also includes a deep reflector (R4) at 871 mbsf.

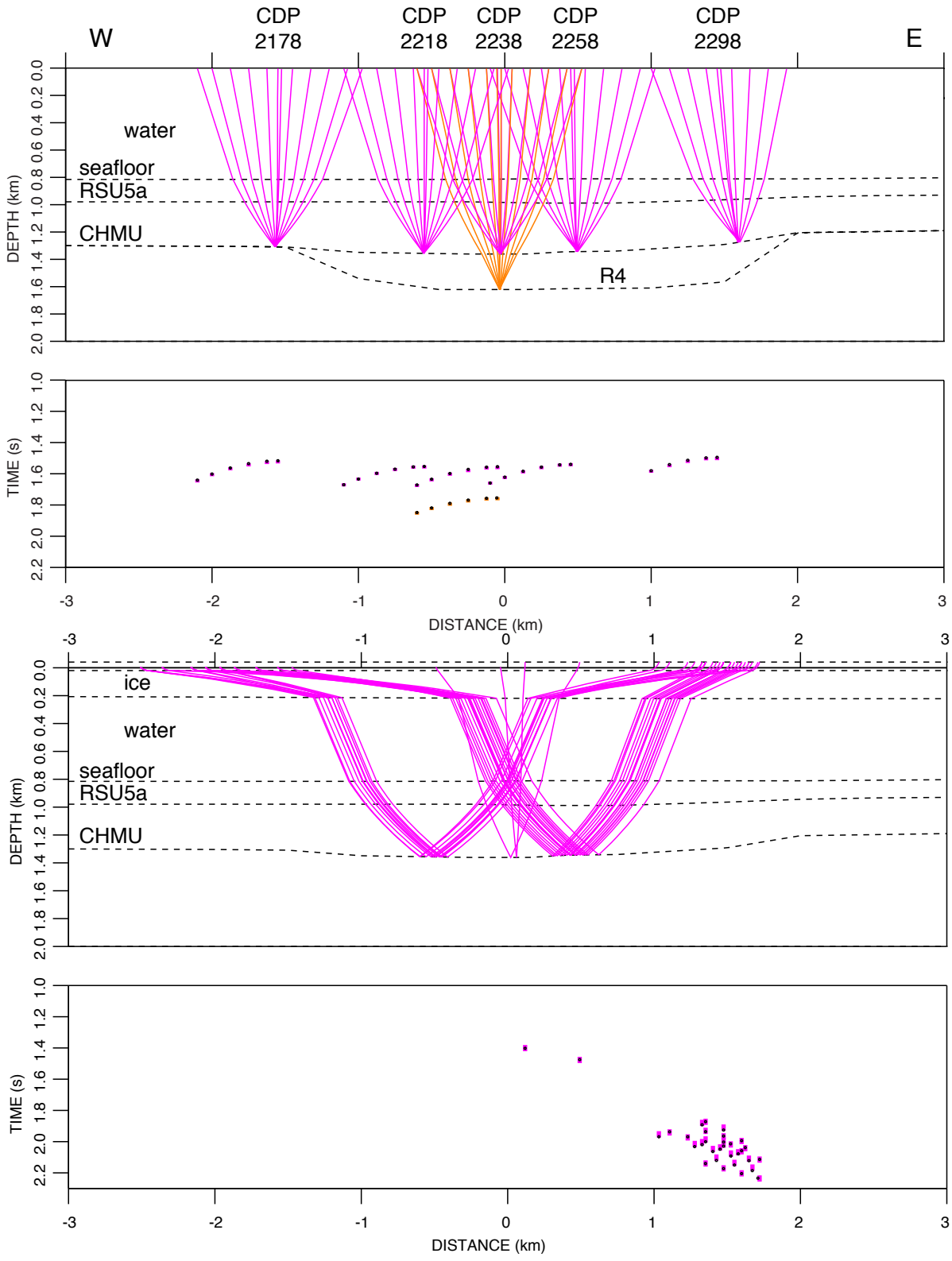

Figure 11. Ray-trace model for CHMU reflections near proposed drill site CH-1 for 2003 NBP0301 MCS data (top) and 2010 over-ice data (bottom). Colored bars for observed travel time are ± 10 ms for MCS and ± 20 ms for over-ice data. This model tests the slow and shallow limit with CHMU at 547 mbsf. The MCS model also includes a deep reflector (R4) at 807 mbsf.

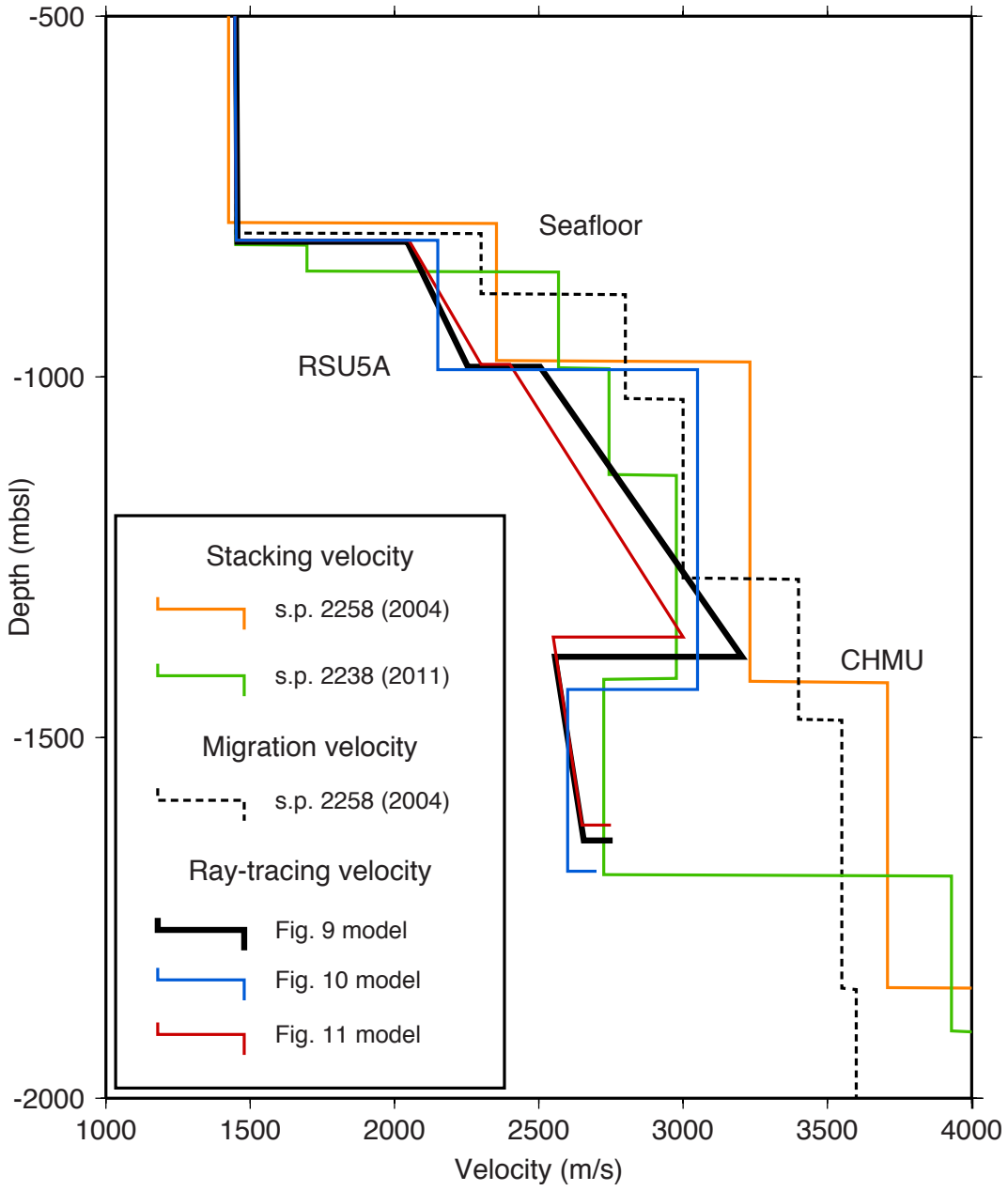

Figure 12. Contrasting velocity-depth functions near proposed drill site CH-1. Stacking velocities (from MCS) are interval velocities from semblance analysis and the Dix equation, from initial bulk processing (orange) and recent careful reinterpretation (green). Migration velocity (dashed) is a regionally smoothed version of the initial interval stacking velocities. Ray-tracing velocities show models satisfying both MCS and over-ice data, with contrasting versions for best-fit (Fig. 9), fast-deep limit (Fig. 10), and shallow-slow limit (Fig 11). The best-fit depth to Coulman High Major Unconformity (CHMU) is 575 mbsf, range is 547-619 mbsf. Velocities deeper than ~1700 mbsl are poorly constrained.